Journal of Physics and Chemistry of Solids 74 (2013) 311–314

Contents lists available at SciVerse ScienceDirect

Journal of Physics and Chemistry of Solids

journal homepage: www.elsevier.com/locate/jpcs

# Infrared photoresponse from *pn*-junction $Mg_2Si$ diodes fabricated by thermal diffusion

Haruhiko Udono [a,]*, Yusuke Yamanaka [a], Masahito Uchikoshi [b], Minoru Isshiki [b]

[a] Graduate School of Science and Engineering, Ibaraki University., 4-12-1 Nakanarusawa, Hitachi 316-8511, Japan
[b] IMRAM, Tohoku University, 1-1-2 Katahira, Aoba-ku, Sendai 980-8577, Japan

ARTICLE INFO

*Article history:*
Received 3 September 2012
Received in revised form
9 October 2012
Accepted 15 October 2012
Available online 24 October 2012

*Keywords:*
A. Inorganic compounds
B. Crystal growth
D. Electrical properties
D. Optical properties

ABSTRACT

We fabricated *pn*-junction diodes by thermal diffusion of Ag acceptor into *n*-type melt-grown $Mg_2Si$ single-crystalline substrates (electron concentration $=2\times10^{15}$ $cm^{-3}$) to investigate the infrared photoresponse of the material. The estimated hole concentration at the *p*-side of the diode diffused with Ag at 550 °C was $3\times10^{18}$ $cm^{-3}$. Current–voltage measurement of the diodes showed sound rectifying characteristics even at 300 K. A clear photoresponsivity with a photon energy threshold of approximately 0.6 eV was observed from the diode, showing promise for application in infrared light detection devices at wavelengths of 1.2–2 μm.



## 1. Introduction

Infrared light detection using Si-VLSI-compatible, abundant, and nontoxic materials is attracting increasing attention for applications in Si-photonics, multi-junction solar cells, thermophotovoltaics, and molecular sensing [1–5]. Magnesium silicide ($Mg_2Si$) is one of the candidate materials for Si-based photodetectors operating at wavelengths in the infrared region, because it has an energy gap of $E_g=0.6$ eV, a small lattice mismatch with Si ($<2\%$), an abundance of resources, and a potential for band gap engineering in the narrow band gap range (0.3–0.6 eV) in the form of alloy compounds with $Mg_2Ge$ and $Mg_2Sn$ [6–9].

There have been several authoritative works on the fundamental electrical and optical properties of $Mg_2Si$. Morris et al. precisely investigated the electrical properties of single crystals at 77 K and 1000 K [10]. Koenig et al. reported the indirect-gap nature of $Mg_2Si$ [11]. Stella et al. investigated the absorption spectrum under pressure and reported that the most reliable indirect-gap energy is about 0.59–0.60 at 90 K [12]. Labotz et al. and Zaitsev et al. reported band gap narrowing in $Mg_2Si_xGe_{1-x}$ and $Mg_2Si_xSn_{1-x}$ alloy compounds, respectively.[9,13]. Furthermore, thin film layers of $Mg_2Si$ on Si substrates grown by reactive deposition epitaxy (RDE), molecular beam epitaxy (MBE), ion-beam synthesis (IBS), pulsed laser deposition (PLD), and sputtering have been investigated intensively [14–18].

In contrast, there have been a limited number of reports on the photoresponse of $Mg_2Si$. Stella and Lynch demonstrated photoconductivity of $Mg_2Si$ and $Mg_2Ge$ at low temperatures ($<90$ K) [7]. They observed a photon energy threshold of approximately 0.6 eV for bulk $Mg_2Si$. Kato et al. observed the change in conductivity of a $Mg_2Si$ layer on a Si substrate under simulated AM1.5G illumination. [18] However, the photoresponse from a $Mg_2Si$ pn-junction diode has not been reported so far. Recently, we successfully grew a high-purity $Mg_2Si$ bulk single crystal with an electron concentration of $10^{15}$ $cm^{-3}$ using high-purity Mg and Si source materials and an impervious graphite crucible [5] and also succeeded in obtaining the Au/*n*-$Mg_2Si$ Schottky junction [19].

In the present study, we fabricated a $Mg_2Si$ pn-junction diode by a thermal diffusion process and observed the photoresponsivity with a photon energy threshold at approximately 0.6 eV.

## 2. Experimental

Single-crystalline *n*-type $Mg_2Si$ substrates ($n_{sub}=2\times10^{15}$ $cm^{-3}$, 5–10 Ωcm) were prepared from $Mg_2Si$ ingots grown by a modified vertical Bridgman method using high-purity source materials of Si (10 N-grade, Furuuchi Chemical Co.) and Mg (5 N-grade, Osaka Asahi Co., Ltd.) and purified pyrolytic graphite (PG) crucibles (Ibiden Co.) [5,19]. The $(4–5)\times(3–5)$ $mm^2$, 1-mm-thick $Mg_2Si$ substrates were polished on both sides by fumed silica (AKASEL, water-free, 0.2 μm). A diffusion source of Ag metal (3 N-grade, Nilaco Co.) was evaporated onto the as-polished surface through a

* Corresponding author. Tel./fax: +81 294 38 5126.
*E-mail address:* udono@mx.ibaraki.ac.jp (H. Udono).

0022-3697/$ - see front matter © 2012 Elsevier Ltd. All rights reserved.
http://dx.doi.org/10.1016/j.jpcs.2012.10.005

metal mask with 0.8-mm-diameter holes using a conventional resistive heating evaporator. After this deposition of Ag, a thick Au layer was evaporated on the Ag metal as a capping metal and an ohmic electrode for *p*-$Mg_2Si$. In order to diffuse the Ag-dopant and form a *p*-type region on the *n*-$Mg_2Si$ substrate, the substrate was annealed in an Ar gas flow atmosphere using a rapid thermal annealing (RTA) furnace. The thermal annealing temperature was varied at 450, 500, 550, and 600 °C. The diffusion depth of Ag was evaluated by back-scattered electron imaging and X-ray analysis of the polished surface at a 3° off-angle through scanning electron microscopy combined with energy-dispersive X-ray spectroscopy (SEM-EDX, JEOL JSM-5600LV). Quantitative depth profiles of Ag were also analyzed through secondary ion mass spectroscopy (SIMS). An ohmic contact was formed at the bottom side of the *n*-$Mg_2Si$ substrate using Ag adhesive (DuPont 4922). The photo-response properties of the $Mg_2Si$ *pn*-junction diodes were measured under a zero bias condition using a halogen lamp chopped and passed through a 2-mm-thick Si filter and a single monochromator (JASCO CT-50) with a focal length of 500 mm.

## 3. Results and discussion

Fig. 1(a) shows a typical $Mg_2Si$ substrate cut out with a diamond blade saw from the bulk crystal (12 mm in diameter). The surface was mirror-like, and the typical surface roughness, in terms of the arithmetic average of the absolute values of $R_a$, was 30 nm. After deposition of the Ag source and Au capping layer, the substrate was annealed in the RTA furnace. Fig. 1(b) shows the surface of a *pn*-junction diode fabricated by RTA at 550 °C for 30 min. The surface of the $Mg_2Si$ substrate and Au ohmic electrode had a mirror-like face even after annealing. Above the annealing temperature of 600 °C, the substrate surface became hazy with a dark grayish color, suggesting the vaporization of Mg and surface oxidation with residual gas.

Fig. 2(a) and (b) shows the current–voltage (*J*–*V*) characteristics of the $Mg_2Si$ pn-junction diode prepared by RTA between 450 and 550 °C for 30 min and a schematic illustration of the measurement system, respectively. A clear rectifying behavior of the $Mg_2Si$ diode annealed at 550 °C indicates the formation of a potential barrier and a depletion region at the *pn*-junction of $Mg_2Si$. In contrast, below the annealing temperature of 500 °C, clear rectifying behavior was not observed due to the difficulty of the reliable Ag-diffusion.

Fig. 3 plots the relationship between the annealing period and the Ag diffusion depth of the *pn*-junction diodes at a constant annealing temperature of 550 °C. The diffusion depth was determined through SEM–EDX observations of the polished *pn*-junction at a 3° off-angle. The detection limit of the Ag contrast was approximately $1 \times 10^{19}$ cm$^{-3}$ (inset of Fig. 3). The diffusion depth increased as a square root of the annealing period. If we assume that Ag diffusion occurs under a constant surface concentration condition with the saturation concentration $N_0$, the diffusion depth $W$ is given by [20]

$$W = 2\sqrt{Dt} \times \mathrm{erfc}^{-1}\left(\frac{N_{BC}}{N_0}\right) \quad (1)$$

where $D$ is the diffusion coefficient; $t$, the annealing period; and $N_{BC}$, the Ag concentration at the contrast edge. From the SIMS analysis (described later) and the detection limit of the Ag contrast,

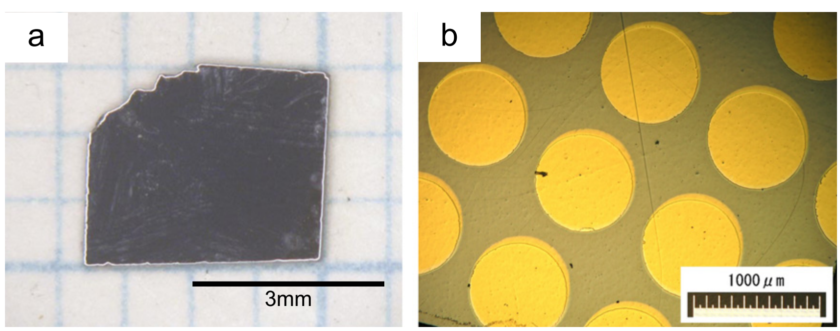


**Fig. 1.** (a) Microphotograph of typical $Mg_2Si$ substrate prepared from a Bridgmann grown single crystalline ingot and (b) top view of a *pn*-junction $Mg_2Si$ diode after RTA at 550 °C for 30 min. Diameter of the gold electrode is 0.8 mm.

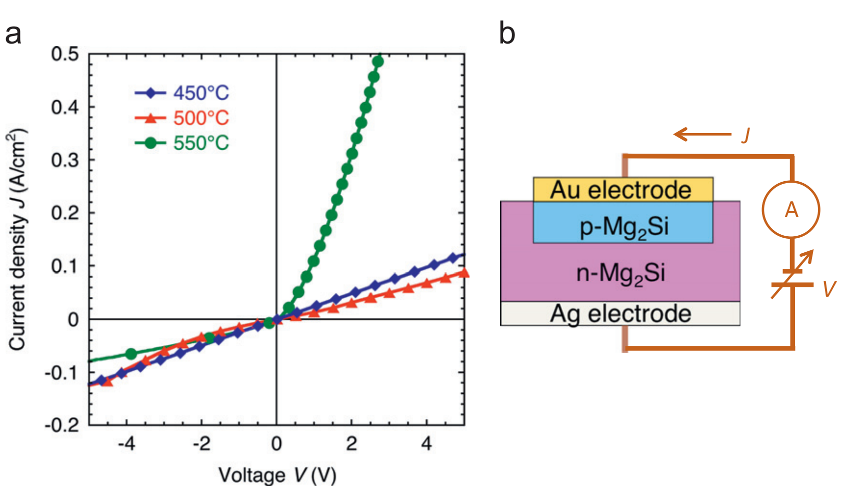


**Fig. 2.** (a) Current–voltage characteristics of *pn*-junction $Mg_2Si$ diodes prepared by RTA between 450 and 550 °C for 30 min. The measurement was carried out at 300 K and (b) cross-sectional schematic illustration of *pn*-junction $Mg_2Si$ diode.

we obtained $N_0 = 2 \times 10^{19}$ cm$^{-3}$ and $N_{BC} = 1 \times 10^{19}$ cm$^{-3}$, respectively. The Ag-diffusion coefficient of $D_{Ag}$ was estimated to be $5 \times 10^{-9}$ cm$^2$/s by fitting the diffusion depth data to Eq. (1) as plotted in Fig. 2. This value is comparable with the interdiffusion coefficients reported for the $Mg_2Si$ growth on Si ($3 \times 10^{-10}$ cm$^2$/s) and the $Mg_2Ge$ growth on Ge ($2 \times 10^{-10}$ cm$^2$/s) [21].

Fig. 4(a) shows the SIMS depth profiles of the diffused Ag acceptor in the $Mg_2Si$ diode annealed at 550 °C for 10 min. The concentration of only the Ag level was calibrated using Ag-doped bulk $Mg_2Si$ crystals grown from the melt. The ion intensities of the main components of Mg and Si were kept constant in the measurement region, indicating that the composition of Mg/Si was unchanged from the bulk composition after the RTA process. The concentration of Ag was $2.0 \times 10^{19}$ cm$^{-3}$ at the surface and $1.7 \times 10^{19}$ cm$^{-3}$ at a depth of 10 μm, which is in agreement with the calculated Ag diffusion profiles using the obtained $D_{Ag}$ (dashed line in Fig. 4(a)). According to our electrical measurements of the Ag-doped melt-grown $Mg_2Si$ bulk crystals [22], the activation ratio of Ag was almost constant at approximately 0.15 between the Ag concentration of $1 \times 10^{17}$ and $1 \times 10^{20}$ cm$^{-3}$ (Fig. 4(b)). Thus, we can estimate that the hole concentration in the Ag diffusion region in Fig. 4(a) was approximately $3 \times 10^{18}$ cm$^{-3}$.

Since the substrate has a low electron concentration and the thermally diffused Ag-dopant shows a gradient profile, the actual pn-junction would locate below the observed contrast edge in Fig. 3. The pn-junction depth where the hole concentration becomes equal to the electron concentration of the substrate was estimated at approximately 83 μm for the diode annealed at 550 °C for 10 min by using the calculated Ag-diffusion profile and the dopant activation ratio. For better understanding the junction property, we also calculated the width of depletion region assuming the step junction ($p^+ = 3 \times 10^{18}$/ $n = 2 \times 10^{15}$ cm$^{-3}$) and a linearly graded junction. The values were approximately 1 μm and 2 μm for a step junction and linearly graded junction, respectively.

Fig. 5 shows the low temperature $J$–$V$ characteristics of the $Mg_2Si$ pn-junction diode prepared by RTA at 550 °C for 10 min. In a forward bias, the $J$–$V$ characteristics at low levels of injection ($V < \sim 0.5$ V) exhibited an exponential behavior. The diode ideality factors $n$ were 2.8 at 300 K, 2.7 at 180 K, and 2.4 at 100 K. These values of $n$ do not fall within the range that results when the diffusion current ($n = 1$) or the recombination current ($n = 2$)

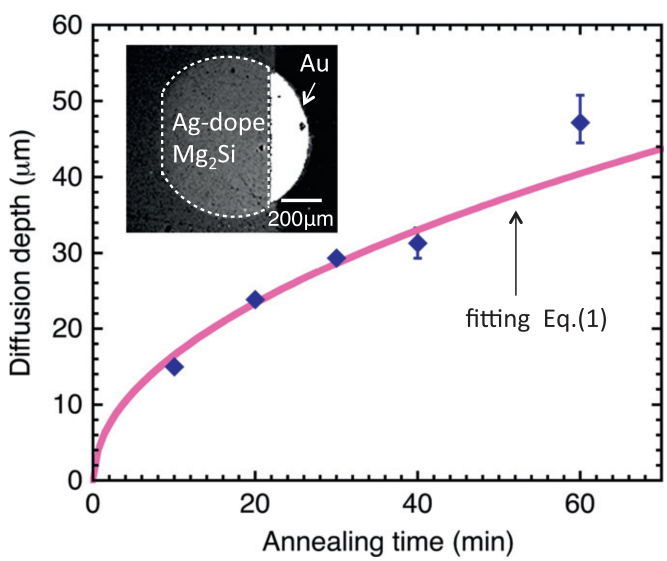


**Fig. 3.** Relationship between the annealing period and the Ag-diffusion depth of the *pn*-junction diodes at a constant annealing temperature of 550 °C. The fitting curve was calculated using Eq. (1), and the obtained diffusion constant $D_{Ag} = 5 \times 10^{-9}$ cm$^2$/s. The inset is the typical back scattered electron image of the *pn*-junction polished at 3° off-angle.

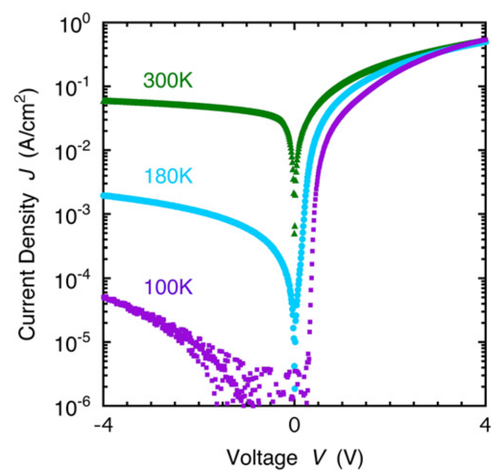


**Fig. 5.** Low temperature current–voltage characteristics of a *pn*-junction $Mg_2Si$ diode prepared by RTA at 550 °C for 10 min. The measurement temperature was varied between 100 and 300 K.

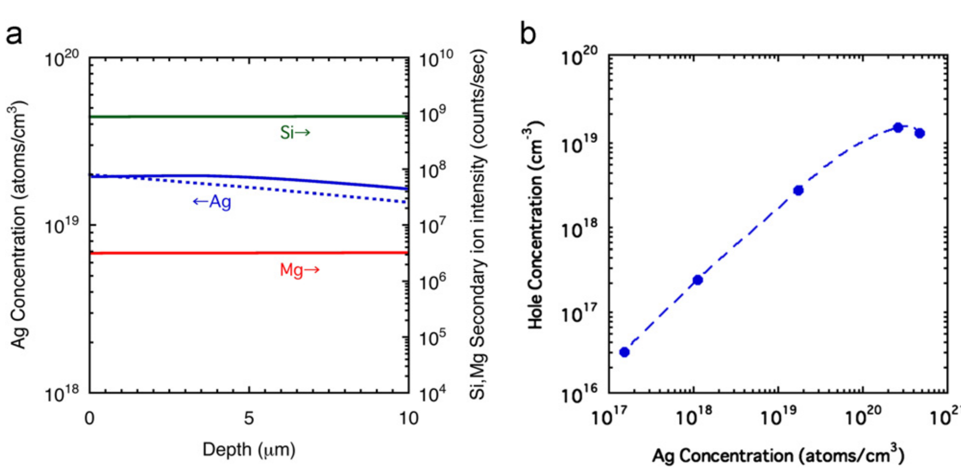


**Fig. 4.** (a) SIMS depth profiles of Mg, Si, and Ag concentrations from the substrate surface of the *pn*-junction diode prepared by RTA at 550 °C for 10 min. Only the Ag concentration was calibrated using an Ag-doped bulk standard and (b) Relationship between Ag-dopant concentration and hole concentration of $Mg_2Si$ crystal at 300 K.

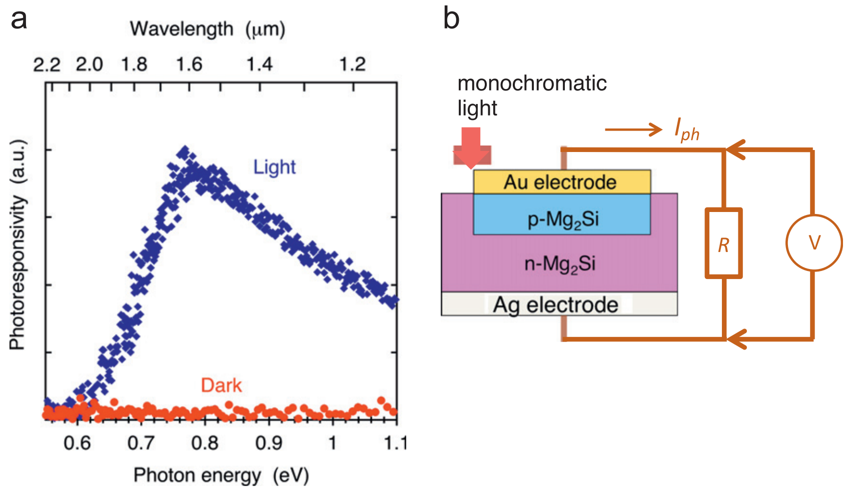


**Fig. 6.** (a) Spectral responsivity of a *pn*-junction $Mg_2Si$ diode under a 0-V bias and (b) measurement circuit of spectral responsivity of the diode. Photocurrent $I_{ph}$ was detected as a voltage between the fixed resistor of $R=1$ kΩ.

dominates the forward bias current conduction. At high voltages ($V>\sim0.5$ V), the series resistance effect appears to dominate.

In a reverse bias, saturation behavior of current density was observed below the bias voltage of $V\sim-1$V. The reverse bias current density at $V=-4$V was 0.06 A/cm$^2$ at 300 K and it decreased to $2\times10^{-3}$ A/cm$^2$ at 180 K and $5\times10^{-5}$ A/cm$^2$ at 100 K. The decrease of reverse bias current density is mainly due to decrease in the minority carrier concentration in *n*-$Mg_2Si$, since the electron concentration of $Mg_2Si$ substrate ($n_{sub}=2\times10^{15}$ cm$^{-3}$) was almost constant between 300 K and 100 K.

Fig. 6(a) shows a typical photoresponse spectrum of a *pn*-junction $Mg_2Si$ diode measured under a non-bias condition at 300 K. Incident monochromatic light was mainly detected at the side edge of *p*-$Mg_2Si$ region because the Au-electrode was nontransparent (Fig. 6(b)). The photocurrent $I_{ph}$ was observed for a photon energy greater than approximately 0.6 eV, and it increased sharply with the increase in the photon energy. These results indicate that the strong electric field in depletion layer at the *pn*-junction effectively separates the electron–hole pairs that are generated by the photo-incidence.

The photon energy threshold at approximately 0.6 eV is the same as that observed for photoconductivity (0.6 eV at 90 K) by Stella and Lynch [7] and is also close to the fundamental absorption edge (0.615 eV at 300 K) determined by Tamura et al. through optical absorption measurements using high-purity $Mg_2Si$ bulk single crystal [6]. In $Mg_2Si$, the exact band-gap energy at room temperature is still controversial since clear phonon structures (phonon emission and absorption) have not been observed in its absorption spectra. The reports so far have shown that the energy gap at room temperature varies between 0.59 eV and 0.67 eV [5,7,9–12]. Our results showing a clear photoresponse above 0.6 eV in *pn*-junction diodes using the high-purity bulk $Mg_2Si$ lead to the following definitive conclusion: a photodiode of $Mg_2Si$ is useful to detect light at wavelengths of 1.2–2 μm.

## 4. Conclusions

We have demonstrated infrared optical detection at wavelengths of 1.2–2 μm using a *pn*-junction diode fabricated by thermal diffusion of an Ag acceptor into *n*-type melt-grown $Mg_2Si$ single-crystalline substrates (electron concentration$=2\times10^{15}$ cm$^{-3}$). The hole concentration estimated using the activation coefficient of Ag-doped bulk $Mg_2Si$ (0.15) and solid solubility of Ag in $Mg_2Si$ at 550 °C ($2\times10^{19}$ cm$^{-3}$) was $3\times10^{18}$ cm$^{-3}$. The current–voltage (*J*–*V*) characteristics of the $Mg_2Si$ *pn*-junction diode showed a clear rectifying behavior. Photoresponsivity measurements revealed that the photon energy threshold of the pn-junction $Mg_2Si$ diode was approximately 0.6 eV at 300 K, showing promise for application in infrared light detection devices.

## Acknowldgments

This work was supported in part by Grants-in-Aid for Scientific Research from the Ministry of Education, Culture, Sports, Science and Technology of Japan (MEXT). The authors would like to thank Dr. M. Nakamura for fruitful discussion.

## References

[1] D. Feng, S. Liao, P. Dong, N. Feng, H. Liang, D. Zheng, C. Kung, J. Fong, R. Shafiiha, J. Cunningham, A.V. Krishnamoorthy, M. Asghari, Appl. Phys. Lett. 95 (2009) 261105.
[2] Q. Xu, B. Schmidt, S. Pradhan, M. Lipson, Nature 435 (2005) 325.
[3] M. Konagai, Jpn. J. Appl. Phys. 50 (2011) 030001.
[4] T.J. Coutts, Sol. Energ. Matter Sol. Cells 66 (2001) 443.
[5] H.R. Herschman, Science 302 (2003) 605.
[6] D. Tamura, R. Nagai, K. Sugimoto, H. Udono, I. Kikuma, H. Tajima, I.J. Ohsugi, Thin Solid Films 515 (2007) 8272.
[7] A. Stella, D.W. Lynch, J. Phys. Chem. Solids 25 (1964) 1253.
[8] K.S. An, R.J. Park, J.S. Kim, C.Y. Park, S.B. Lee, T. Abukawa, S. Kono, T. Kinoshita, A. Kakizaki, T. Ishii, J. Appl. Phys. 78 (1995) 1151.
[9] R.J. LaBotz, D.R. Mason, D.F. O'Kane, J. Electrochem. Soc. 110 (1963) 127.
[10] R.G. Morris, R.D. Redin, G.C. Danielson, Phys. Rev. 109 (1958) 1909.
[11] P. Koenig, D.W. Lynch, G.C. Danielson, J. Phys. Chem. Solids 20 (1961) 122.
[12] A. Stella, A.D. Brothers, R.H. Hopkins, D.W. Lynch, Phys. Status Solidi 23 (1967) 697.
[13] V.K. Zaitsev, E.N. Nikitin, E.N. Tkalenko, Sov. Phys. Solid State 11 (1969) 3000.
[14] J.E. Mahan, A. Vantomme, G. Langouche, Phys. Rev. B 54 (1996) 16965.
[15] W.K. Chu, S.S. Lau, J.W. Mayer, H. Muller, Thin Solid Films 25 (1975) 393.
[16] M. Baleva, G. Zlateva, A. Atanassov, M. Abrashev, E. Goranova, Phys. Rev. B 72 (2005) 115330.
[17] S. Song, K.A. Striebel, X. Song, E.J. Cairns, J. Power Sources 119 (2003) 110.
[18] T. Kato, Y. Sago, H. Fujiwara, J. Appl. Phys. 110 (2011) 063723.
[19] K. Sekino, M. Midonoya, H. Udono, Y. Yamada, Phys. Procedia 11 (2011) 171.
[20] E.S. Yang, Fundamentals of Semiconductor Devices, McGraw-Hill, New York, 1978.
[21] Y. Mizuyoshi, R. Yamada, T. Ohishi, Y. Saito, T. Koyama, Y. Hayakawa, T. Matsuyama, H. Tatsuoka, Thin Solid Films 508 (2006) 70.
[22] H. Udono, K. Kushida, H. Koguchi, Abtracts Book of The International Conference on Thermoelectrics, C.a.5, 2008 Oregon, USA.